Journal of Electrical Engineering & Technology
https://doi.org/10.1007/s42835-020-00498-3

ORIGINAL ARTICLE

Design of a Wideband Coupled Feed Dipole Antenna for PCL Array Systems

Sungsik Wang[1] · Junsik Park[2] · Hongsuk Shim[2] · Hosung Choo[1]

Received: 26 April 2020 / Revised: 4 June 2020 / Accepted: 28 July 2020

Abstract
This article proposes the design of a wideband coupled feed dipole antenna for Passive Coherent Location (PCL) systems. The proposed antenna consists of an internal direct feed dipole and an external coupled feed dipole. This coupled feed mechanism, which is often used in microstrip patch antennas, is applied to the dipole element for a wide matching bandwidth. To verify the operating principle of the proposed antenna, an equivalent circuit model is investigated along with some parametric studies of the coupling effect. The proposed antenna is then extended to an eight-element uniform circular array to confirm the beamforming performance for PCL systems. The results demonstrate that the coupled feed dipole element is more suitable to enhance the matching bandwidth compared to a conventional dipole antenna.

Keywords PCL antennas · FM · Array antennas · Broadband antennas · Multiband antennas

1 Introduction

Passive coherent location (PCL) systems are bistatic radars using commercial broadcasting signals including FM radio [1, 2] analog TV [3], digital TV [4–7] mobile communications [8], and satellite [9, 10]. PCL systems do not require additional transmitters unlike other typical active radars, which has the advantages of minimizing the exposure of observation sites while increasing the detection accuracy by multiple observation sites at a low cost. In addition, the use of the VHF frequency band allows PCL systems to detect long-range targets and counteract stealth technologies, such as RCS reduction and low altitude flight [11–13]. Many studies have been extensively conducted and reported to improve the PCL system performance in various ways. Among them, there have been several efforts to enhance detection performance by improving the signal processing algorithms. Techniques for enhancing the detection efficiency using Doppler-sensitive cross-correlation has been studied [1], and recently, methods of mitigating interference, such as the multipath and clutter echoes by canceling sequential zero-Doppler signal components have also been proposed [14, 15]. On the other hand, some studies have focused on deriving the proper transmitter waveforms by checking self-ambiguity [16, 17], and efforts have also been made to increase received information in various ways, such as using polarization diversity [18, 19], spatial diversity [20], multistatic transmitters [6, 21], and multistatic receivers [4, 22]; however, these previous efforts mainly focused on performance improvement in terms of algorithms and software—not the hardware of antenna elements that can further improve system performance. In particular, the PCL system should be able to receive a variety of commercial radio sources so that the broad matching bandwidth of the receiving antenna with an omni-directional pattern is one of the key factors in determining overall system performance. Although there were some previous studies on broadband dipole antennas [23, 24], they were not suitable for PCL system applications in terms of frequency or outdoor installation. The dual-band antenna of PCL systems has recently been reported to improve the system detection area, but the bandwidth of each band is limited, and the work is mainly focused on ARD maps through the ambiguity function [6].

✉ Hosung Choo
hschoo@hongik.ac.kr

Sungsik Wang
kingwss@gmail.com

Junsik Park
juneg@hanwha.com

[1] School of Electronic and Electrical Engineering, Hongik University, Seoul 121-791, Republic of Korea

[2] Hanwha Systems Co. Ltd, Seongnam, Korea

Published online: 10 August 2020

In this paper, a novel design of an array element that can achieve a wide matching bandwidth by applying a coupled feed mechanism to a dipole antenna is proposed. This coupled feed, which is often used in microstrip patch antennas [25–27], is applied to the broadband dipole element for PCL systems. The antenna element consists of an internal direct feed dipole and an external coupled feed dipole. These internal and external dipoles are fixed by the housing structure that employs the circuit board of a balun. The proposed structure allows two adjacent resonances to be placed close to each other to achieve broadband characteristics, and it can also adjust the operating frequency by simply replacing the external dipole according to the system requirements. To verify the feasibility of the proposed design, the coupled feed dipole element is fabricated, and the antenna characteristics, such as the bore-sight gains and reflection coefficients, are measured. In addition, to analyze the operating principle of the proposed antenna design, an equivalent circuit model of the antenna is investigated along with some parametric studies of the coupling effect between the internal and external dipoles. The proposed antenna element is then extended to an 8-element circular array, and the beamforming performance of the array is examined. The results demonstrate that the proposed coupled feed dipole achieves better array antenna characteristics compared to the conventional basic dipole array.

2 Proposed Antenna Structure

Figure 1 shows the proposed broadband dipole antenna with an electromagnetically coupled feed structure. The antenna consists of internal and external dipoles with a radius of R_{in} and R_{out}, respectively. The internal dipole is fed directly from the circuit board with the embedded balun, and the external dipole is electromagnetically coupled to the internal dipole to achieve the broadband matching characteristics. This coupled feed structure is conceptually similar to the coupling feeding mechanism often employed in dual-band microstrip patch antennas; however, for this work, the feeding mechanism is applied to the design of broadband dipole antennas for the FM frequency band. The coupled feed mechanism used for the broadband dipole element can dramatically improve the matching characteristics, which can enhance the overall performance of PCL systems. The internal and external dipoles have an indirect feeding structure with a separation gap of S_{d1}, and an air gap without a dielectric material is filled between the two radiators to ensure no dielectric loss. The lengths of the internal and external dipole radiators are denoted by H_{out} and H_{in}, respectively, and each of these parameters determines the resonance frequency. The resonance characteristics can also vary slightly depending on the parameters of R_{in} and R_{out}, as well as S_{d2} that is the gap between the upper and lower dipoles. To derive the optimal parameter values of the proposed antenna, the FEKO EM simulator [28] in conjunction with a genetic algorithm [29] are used. The detail optimized parameters are shown in Table 1.

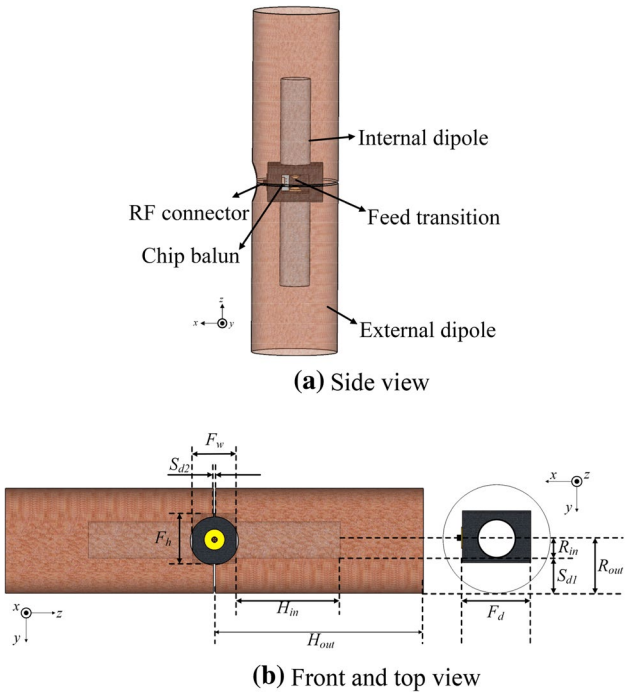

Fig. 1 Geometry of the proposed coupled feed dipole

Table 1 Parameters for the proposed antenna

Parameters	Values (mm)
H_{out}	750
H_{in}	670
R_{out}	62.5
R_{in}	15
S_{d1}	42.5
S_{d2}	1.6
F_w	45
F_d	68
F_h	49

Figure 2 shows the photographs of the proposed coupled feed dipole antenna. The major five components are shown in Fig. 2a, and the housing including the circuit board with the balun is shown in Fig. 2b. The two conducting sticks of the internal dipole, which are surrounded by external dipoles, are firmly attached to the housing by the screw type connectors as shown in Fig. 2c. The fully assembled antenna, including the internal and external radiators, is shown in Fig. 2d. Additional advantage of this design is that the operating frequency of the antenna can be easily adjusted

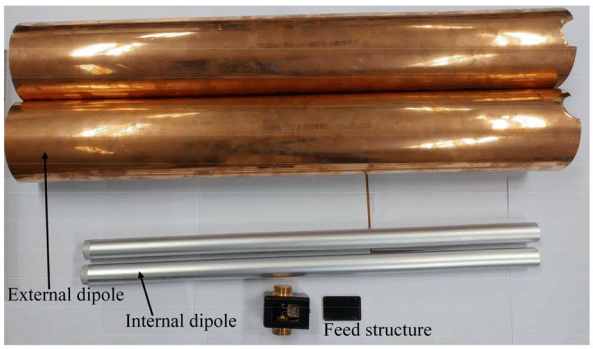

(a) Antenna components

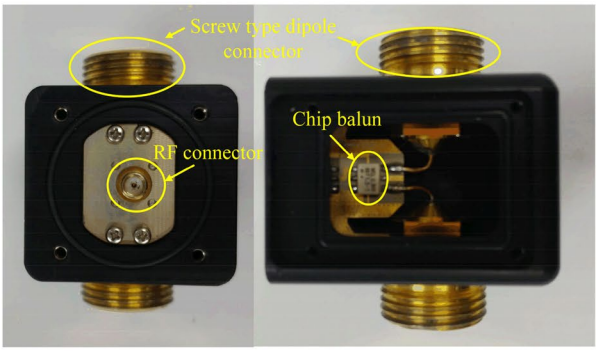

(b) Feed structure

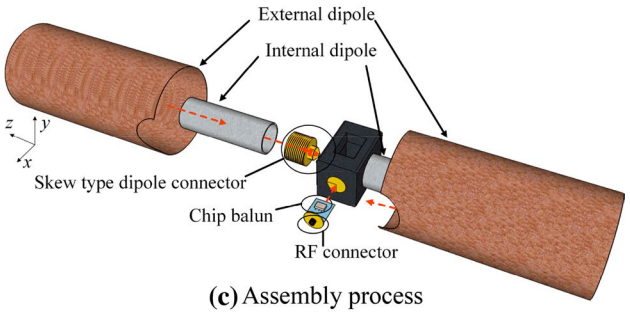

(c) Assembly process

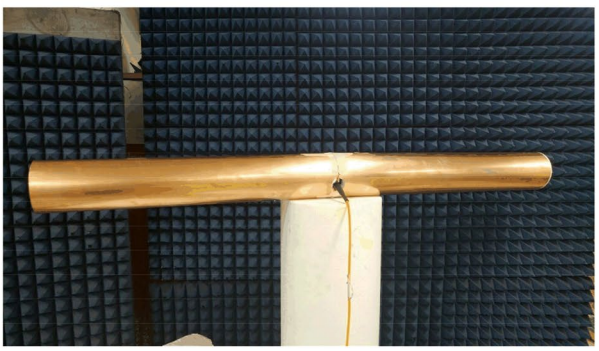

(d) Assembled antenna

Fig. 2 Photographs of the fabricated antenna

by simply replacing the external dipole according to the system requirements. The antenna characteristics, such as the reflection coefficients and bore-sight gains are measured at an outdoor calibration test site.

Figure 3 shows the reflection coefficients of the proposed coupled feed dipole antenna, where the dashed and solid lines present the simulated and measured results, respectively. The − 10 dB matching region is displayed in gray. In addition, the simulated and measured reflection coefficients of the conventional thin dipole, whose geometry information are listed in Table 2, and geometry is shown in Fig. 4, are also provided to compare the proposed feed mechanism. As can be observed, an additional resonance caused by the external radiator occurs beyond the FM region, and the matching characteristics of the proposed antenna show a wide matching bandwidth from 87 to 147.4 MHz (60.4 MHz, $\Gamma < -10$ dB) .

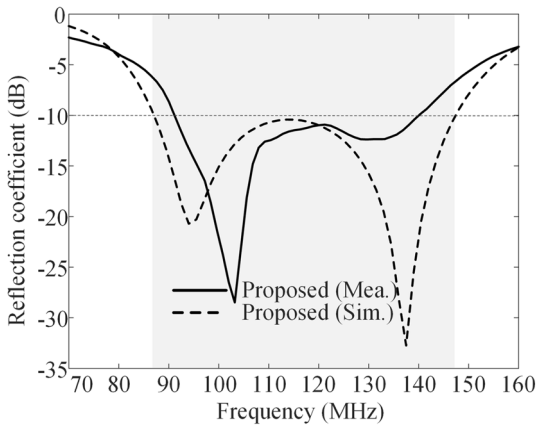

(a) Proposed antenna

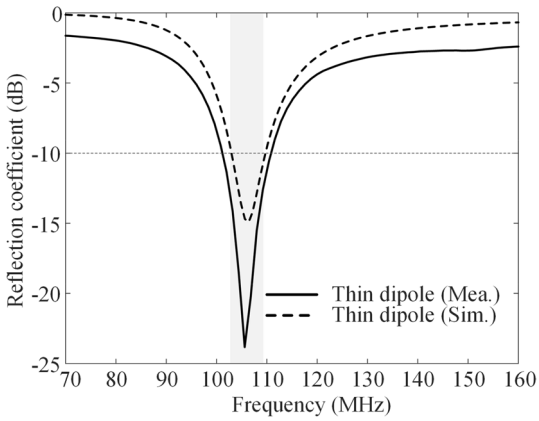

(b) Thin dipole

Fig. 3 Matching characteristic

Table 2 Parameters for the reference antenna

Parameters	Values (mm)
H_{ref}	670
R_{ref}	2
G_{ref}	5

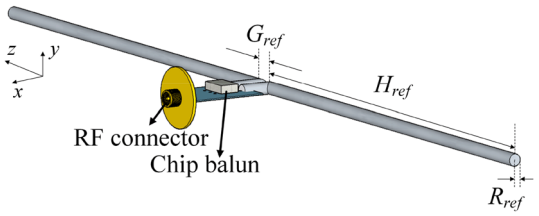

Fig. 4 Geometry of conventional reference dipole

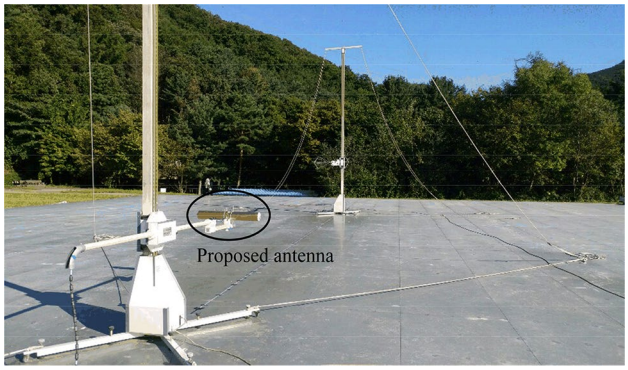

Fig. 5 Outdoor test site supporting CIS16-1-5 standard

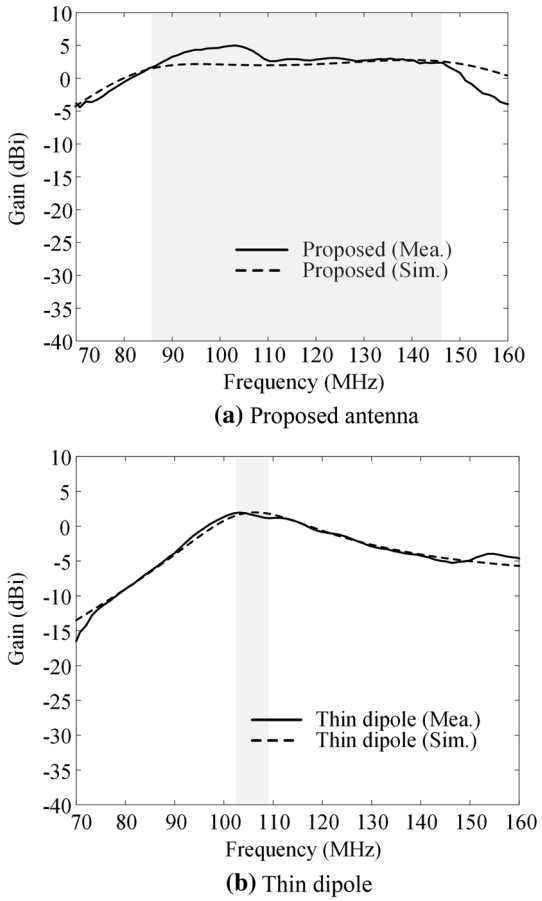

Fig. 6 Bore-sight gain

The radiation characteristics of the fabricated antenna were measured at an outdoor test site, as shown in Fig. 5.

Figure 6 shows the measured bore-sight gains compared with the simulated data. The average gains from 80 to 160 MHz of the proposed antenna are 2.07 dBi by simulation and 2.28 dBi by measurement, which are above 0 dBi over a wide frequency band. In terms of the 3-dB gain bandwidth, the operating frequency range is from 79 to 162 MHz. There are some differences between measurement and simulation. Part of the reason for this difference is that the antenna was measured in an outdoor test site instead of a full anechoic chamber due to the low operating frequency. Another reason for the difference is that the circuit board of the feeding system was not fully included in the EM simulation.

Figure 7 shows the 2-D radiation patterns of the proposed antenna compared with the conventional thin dipole antenna. The proposed antenna has half-power beam widths (HPBWs) of 75.8° and 62.7° at 100 MHz and 140 MHz, respectively, while at the same frequency bands, bore-sight gains of 1.95 dBi and 2.65 dBi are observed. On the other hand, the conventional thin dipole antenna has HPBWs of 79.8° and 70.1° with bore-sight gains of 0.62 dBi and −4.1 dBi, respectively.

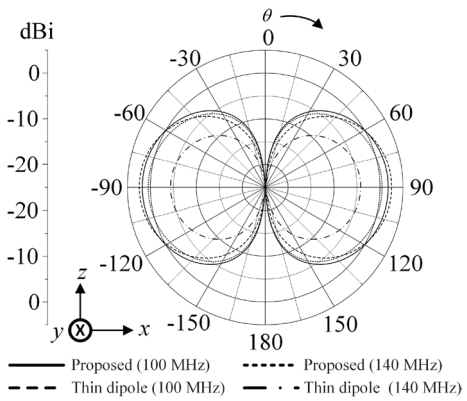

Fig. 7 2-D Radiation patterns in the zx-plane

3 Verification of the Proposed Antenna

3.1 Parametric Study and Analysis

Figure 8 shows the simulated parametric studies of the reflection coefficients according to the heights of the

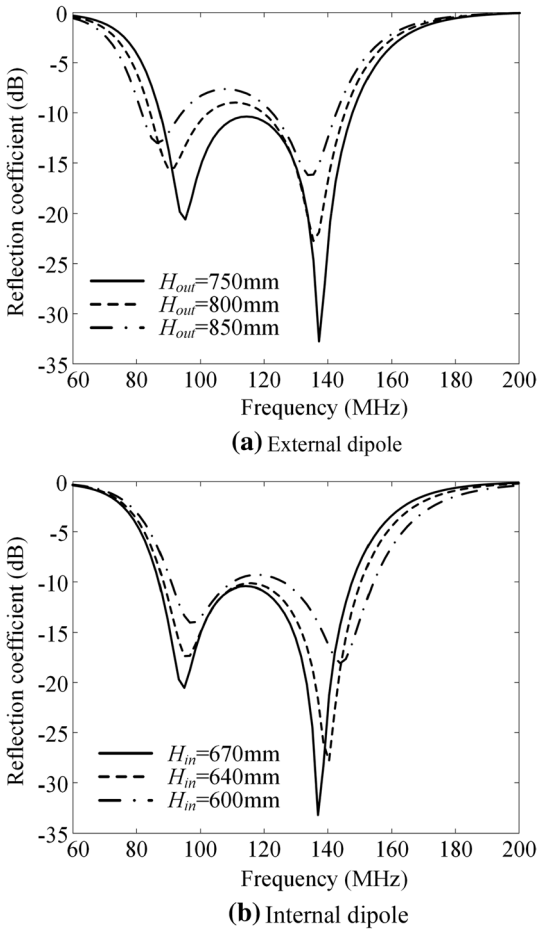

Fig. 8 Reflection coefficients according to the height of the dipole

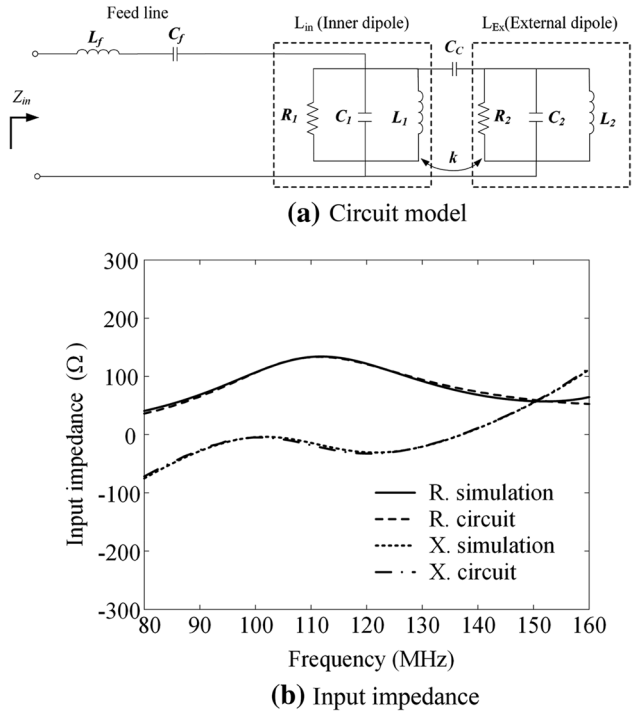

Fig. 9 Equivalent circuit model and its input impedance

internal and external dipoles. Figure 8a illustrates the characteristics of the reflection coefficient according to H_{out} when H_{in} is fixed to 0.67 m. As H_{out} decreases from 850 to 750 mm, the 1st resonance frequency shifts from 85 to 95 MHz, and 2nd resonance frequency shifts from 135 to 137 MHz. As can be observed, the reflection coefficient at the lower resonance frequency changes more, while the higher resonance frequency is relatively less affected. Figure 8b illustrates the reflection coefficient according to H_{in} when H_{out} is fixed to 0.75 m. As H_{in} increases from 600 to 670 mm, the 2nd resonance frequency shifts from 144 to 137 MHz, and 1st resonance frequency shifts from 97 to 95 MHz. Here, in contrast, the reflection coefficient at a higher resonance frequency shifts rapidly, while little change is observed at the lower resonance frequency. These results show that each internal and external dipole generates two adjacent resonances independently, and the broadband characteristic can be achieved by adjusting these two resonances.

To analyze the operating principle of the proposed coupled feed dipole antenna from a circuit perspective, an equivalent circuit model is developed using a data fitting method, as shown in Fig. 9a. The internal dipole can be expressed by a shunt circuit of R_1, L_1, and C_1, and is directly fed by the inductance L_f and capacitance C_f, which represents the feed line [30, 31]. The lumped elements of the external dipole are specified as R_2, L_2, and C_2, and it is fed indirectly through the series coupling capacitance C_c and the inductive coupling coefficient k. The values of C_c and k can be adjusted by gaps (S_{d1} and S_{d2}) and heights (H_{in} and H_{out}). The circuit model parameters are adjusted iteratively to minimize the impedance difference between the circuit model and the simulation. Detailed values of the lumped elements are listed in Table 3, and the input impedance of the equivalent circuit is compared to that of the EM simulation in Fig. 9b.

3.2 Design of 8-Element Uniform Circular Array

To verify the beamforming performance, the proposed coupled feed dipole element is extended to the eight-element uniform circular array (UCA) as presented in Fig. 10. The array distance from the center to the antenna element is $0.5\lambda_0$ with a height of 8 m, and the detailed parameters for the array are listed in Table 4. The PCL system detects the target by using the correlation between the reference and surveillance channels. The reference channel steers the beam to the base station to obtain the commercial broadcast

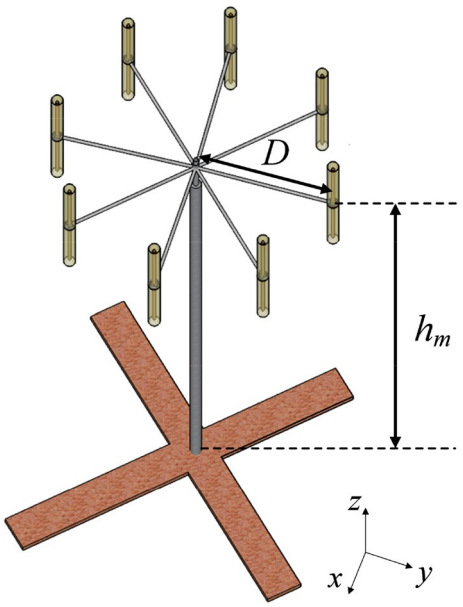

Fig. 10 Array configuration of the PCL system

Table 3 Parameters for the circuit configuration

Parameters	Values
L_f	181.5 nH
C_f	8.18 pF
L_1	111.9 nH
R_1	397 Ω
C_1	1.26 pF
L_2	39.76 nH
R_2	92.2 Ω
C_2	46.57 pF
C_c	14.7 pF
k	0.74
L_f	181.5 nH

signals, while the surveillance channel has a radiation pattern that includes a deep null towards the base station to collect echo signals reflected from targets. Therefore, the steered beam and null patterns are essential performances for the PCL system.

Figure 11 illustrates the reference and surveillance radiation patterns at the center frequency of 100 MHz in the FM band. The beam and null patterns are obtained by extracting the active element pattern (AEP) of each antenna element for the array configuration. The feed weightings for the required steering are optimized using the least-mean-square (LMS) algorithm to derive a narrow half-power beamwidth (HPBW) and a deep null depth. The average peak to side lobe ratio (PSLR) of the reference beam is 18.4 dB, while the average null depth of the surveillance beam is – 37.3 dB.

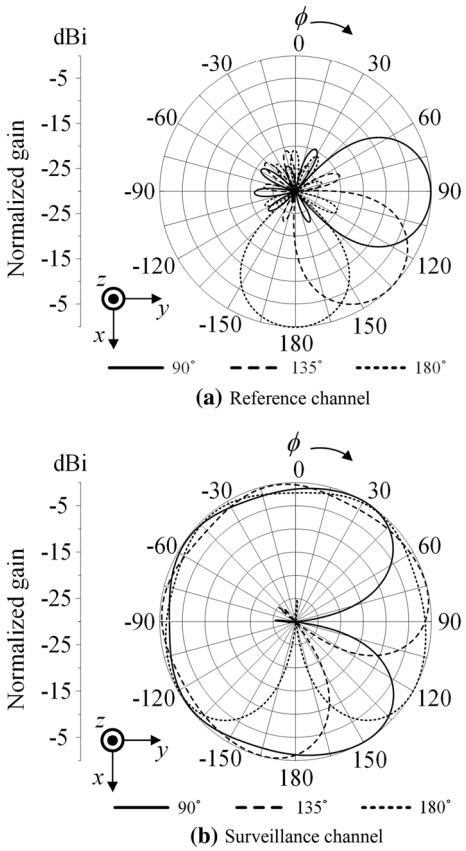

Fig. 11 Optimized radiation patterns

Table 4 Parameters for the array configuration

Parameters	Values
Number of array element	8
Array distance (D)	$0.5\lambda_0$
Mast height (h_m)	8 m
Array type	Uniform circular array

4 Conclusion

The design of a wideband coupled feed dipole antenna for PCL systems was investigated. The proposed antenna, which is composed of internal and external dipoles, can derive the wide matching bandwidth by using an electromagnetically coupled feed mechanism. Antenna characteristics were measured at an outdoor test site to compare the results with the simulation. The reflection coefficients were under – 10 dB from 87 to 147.4 MHz, and the 3-dB gain bandwidth for boresight direction had an operating frequency range from 79 to 162 MHz. To verify the operating

principle of the proposed dipole element, the equivalent circuit was built and analyzed. The results demonstrate that the proposed coupled feed structure can derive the wide matching characteristics by using the series coupling capacitance (C_c) and the inductive coupling coefficient (k). The proposed dipole element was then extended to the 8-element UCA, and it was confirmed that the proposed array had suitable beamforming performance for PCL systems.

Acknowledgements This study was funded by Hanwha syatems.

References

1. Howland PE, Maksimiuk D, Reitsma G (2005) FM radio based bistatic radar. IEE Proc Radar Sonar Navig 152(3):107–115
2. Paine S, O'Hagan DW, Inggs M, Schupbach C, Böniger U (2019) Evaluating the performance of FM-based PCL radar in the presence of jamming. IEEE Trans Aerosp Electron Syst 55(2):631–643
3. Howland PE (1999) Target tracking using television-based bistatic radar. IEE Proc Radar Sonar Navig 146(3):166–174
4. Berger C, Demissie B, Heckenbach J, Willett P, Zhou S (2010) Signal processing for passive radar using OFDM waveforms. IEEE J Sel Top Signal Process 4(1):226–238
5. Colone F, Langellotti D, Lombardo P (2014) DVB-T signal ambiguity function control for passive radars. IEEE Trans Aerosp Electron Syst 50(1):329–347
6. Wang S, Shim H, Choo H (2020) Design and performance prediction of a dual-band coupled-fed dipole array antenna for PCL systems in the VHF band. Appl Sci 10(5):1835
7. Chabriel G, Barrère J (2017) Adaptive target detection techniques for OFDM-based passive radar exploiting spatial diversity. IEEE Trans Signal Process 65(22):5873–5884
8. Stinco P, Greco MS, Gini F, Rangaswamy M (2012) Ambiguity function and Cramér-Rao bounds for universal mobile telecommunications system-based passive coherent location systems. IET Radar Sonar Navig 6(7):668–678
9. Li Z, Santi F, Pastina D, Lombardo P (2017) Passive radar array with low-power satellite illuminators based on fractional fourier transform. IEEE Sens J 17(24):8378–8394
10. Santi F, Pieralice F, Pastina D (2019) Joint detection and localization of vessels at sea with a GNSS-based multistatic radar. IEEE Trans Geosci Remote Sens 57(8):5894–5913
11. Kim IH, Choi IS, Chae DY (2018) A study on the performance enhancement of radar target classification using the two-level feature vector fusion method. J Electromagn Eng Sci 18(3):206–211
12. Shin H, Oh H (2019) UHF-band TV transmitter for TV white space video streaming applications. J Electromagn Eng Sci 19(4):227–233
13. Kuschel H, Heckenbach J, Schell J (2013) Deployable multiband passive/active radar for air defense (DMPAR). IEEE Aerosp Electron Syst Mag 28(9):37–45
14. Colone F, Cardinali R, Lombardo P (2006) Cancellation of clutter and multipath in passive radar using a sequential approach. In: IEEE Radar Conference, Verona, NY, pp 1–7
15. Fu Y, Wan X, Zhang X, Fang G, Yi J (2017) Side peak interference mitigation in FM-based passive radar via detection identification. IEEE Trans Aerosp Electron Syst 53(2):778–788
16. Griffiths HD, Baker CJ (2005) Passive coherent location radar systems. Part 1: performance prediction. IET Proc Radar Sonar Navig 152(3):153–159
17. Griffiths HD, Baker CJ (2005) Passive coherent location radar systems. Part 2: Waveform properties. IET Proc Radar Sonar Navig 152(3):160–168
18. Colone F, Lombardo P (2015) Polarimetric passive coherent location. IEEE Trans Aerosp Electron Syst 51(2):1079–1097
19. Piasecki P, Gasztold M (2015) Dual polarized circular array antenna for PCL system and possibility of digital beamforming of an antenna pattern. In: 2015 European microwave conference (EuMC), Paris, France, pp 119–122
20. Malanowski M, Kulpa K (2008) Digital beamforming for passive coherent location radar. In: 2008 IEEE radar conference, Rome, Italy, pp 1–6
21. Hu P, Bao Q, Chen Z (2019) Target detection and localization using non-cooperative frequency agile phased array radar illuminator. IEEE Access 7:111277–111286
22. Paichard Y, Inggs MR (2009) Multistatic passive coherent location radar systems. In: 2009 Eupopean radar conference (EuRAD), Rome, Italy, pp 45–48
23. Lu WJ, Zhu L, Tam KW, Zhu HB (2017) Wideband dipole antenna using multi-mode resonance concept. Int J Microw Wirel Technol 9(2):365–371
24. Hsu HT, Huang TJ (2012) Generic dipole-based antenna-featuring dual-band and wideband modes of operation. IET Microw Antennas Propag 6(15):1623–1628
25. Byun G, Choo H, Ling H (2013) Optimum placement of DF antenna elements for accurate DOA estimation in a harsh platform environment. IEEE Trans Antennas Propag 61(9):4783–4791
26. Byun G, Hur J, Kang S, Son SB, Choo H (2019) Design of a coupled feed structure with cavity walls for extremely small anti-jamming arrays. IEEE Access 7:17279–17286
27. Byun G, Kim S, Choo H (2014) Design of a dual-band GPS antenna using a coupled feeding structure for high isolation in a small array. Microw Opt Technol Lett 56(2):359–361
28. FEKO EM Simulation Software, Altair Engineering Inc., 2018. https://www.altair.co.kr. Accessed 26 Aug 2019
29. Byun G, Hyun JC, Seo SM, Choo H (2016) Optimum array configuration to improve null steering time for mobile CRPA systems. J Electromagn Eng Sci 16(2):74–79
30. Liao Y, Hubing TH, Su D (2012) Equivalent circuit for dipole antennas in a lossy medium. IEEE Trans Antennas Propag 60(8):3950–3953
31. Tang TG, Tieng QM, Gunn MW (1993) Equivalent circuit of a dipole antenna using frequency-independent lumped elements. IEEE Trans Antennas Propag 41(1):100–103

Sungsik Wang received the B.S. and M.S. degrees in radio science and engineering from Hanyang University, Seoul, Korea, in 1997 and 1999, respectively. He is currently working toward the Ph.D. degree in electronics and computer engineering at Hongik University, Seoul, Korea. His research interests include the Beam propagation under the abnormal atmospheric phenomenon, broadband antenna design, and the use of the optimization algorithm in developing antennas, and antenna arrays beamforming.

Junsik Park received the B.S. and M.S. degrees in Electronics Engineering from Chonbuk National University, Jeonju, Republic of Korea, in 2014 and 2016. He is currently working researcher in Hanwha Systems, Pangyo, Republic of Korea. His research interests include the electric-warfare system, electric support (ES), electric attack (EA) and military antenna & RF circuit.

Hongsuk Shim received the B.S. in Computer Engineering from Chungbuk National University, Cheongju in 2005 and his M.S. degrees in Computer Engineering from Chungnam National University, Daejeon in2008. He is currently working researcher in Hanwha Systems, Pangyo, Korea. His research interests include the electricwarfaresystem, electric support (ES), electric attack (EA) and ELINT/COMINT signal analysis & signal processing.

Hosung Choo received the B.S. degree in radio science and engineering from Hanyang University in Seoul in 1998, and the M.S. and Ph.D. degrees in electrical and computer engineering from the University of Texas at Austin, in 2000 and 2003, respectively. In September 2003, he joined the school of electronic and electrical engineering, Hongik University, Seoul, Korea, where he is currently a full professor.His principal areas of research are the use of the optimization algorithm in developing antennas and microwave absorbers. His studies include the design of small antennas for wirelesscommunications, reader and tag antennas for RFID, and on-glass and conformal antennas for vehicles and aircraft.